BMC Cardiovascular Disorders

RESEARCH

Open Access

Alantolactone mitigates the elevation of blood pressure in mice induced by angiotensin II by inhibiting calcium channel activation

Ruqiang Yuan[1†], Mingjing Gao[2,3†], Hu Xu[4†], Qing Liang[1], Lei Qian[1], Yali Wang[1], Houli Zhang[3*], Erjiao Qiang[5*] and Weijing Yun[1*]

Abstract

Background The dried root of *Inula helenium* L., known as Inulae Radix in Mongolian medicine, is a widely used heat-clearing plant drug within the Asteraceae family. Alantolactone (ATL), a compound derived from Inulae Radix, is a sesquiterpene lactone with a range of biological activities. However, there is a lack of studies investigating its effectiveness in the treatment of hypertension. The aim of this study is to explore the regulatory effect of alantolactone on blood pressure and its underlying mechanism.

Methods and results Network pharmacology analysis suggested that ATL had a potential therapeutic effect on hypertension induced by angiotensin II (Ang II). Subsequently, the results of animal experiments demonstrated that ATL could suppress the increase in blood pressure caused by Ang II. Vascular ring experiments indicated that ATL could inhibit the vascular contractions induced by Ang II, Phenylephrine, and Ca^{2+}. Further experiments demonstrated that ATL could inhibit the calcium influx induced by Ang II and increase the expression of pMLC2. Molecular docking experiments showed that ATL had a high binding affinity with L-type Voltage-gated Calcium Channels (VGCC), and vascular ring experiments indicated that ATL could significantly inhibit the vascular contractions caused by the agonists of L-type VGCC. In addition, we also observed that ATL had an ameliorative effect on the vascular remodeling induced by Ang II.

Conclusions ATL exerted an antihypertensive effect by inhibiting the activation of L-type VGCC and reducing calcium influx.

Keywords Alantolactone, Hypertension, Voltage-gated Calcium Channels, Calcium influx

†Ruqiang Yuan, Mingjing Gao and Hu Xu contributed equally to this work.

*Correspondence:
Houli Zhang
houlizh@163.com
Erjiao Qiang
qiangerjiao@126.com
Weijing Yun
yunweijing@dmu.edu.cn
Full list of author information is available at the end of the article

Introduction

Hypertension is a chronic condition characterized by consistently high blood pressure in the arteries, defined as equal to or greater than 130/85 mmHg [1]. It can divided into two types: essential hypertension and secondary hypertension [2]. Prolonged hypertension has negative effects on various organ systems including the cardiovascular system, cerebrovascular system, kidneys, and vision [3, 4]. Additionally, it increases the risk of developing chronic diseases and significantly impacts both the quality of life and lifespan of affected individuals [5]. Currently, the existing pharmacological interventions for managing hypertension (such as angiotensin-converting enzyme inhibitors, angiotensin II (Ang II) receptor blockers, diuretics, calcium channel blockers, etc.) only provide partial control over the progression of the disease and may potentially lead to drug resistance or metabolic disorders, as well as adverse effects on liver and kidney function [6–8]. Therefore, it is urgently necessary to explore new antihypertensive agents that are both safe and effective.

Blood pressure regulation is influenced by cardiac output (CO) and total peripheral resistance (TPR) [9]. Vasoactive substances secreted by the nervous system and renin angiotensin-aldosterone system (RAAS) can modulate blood pressure by altering CO and TPR, thereby ensuring adequate organ perfusion [10]. Typically, CO remains relatively stable in the body, while TPR increases due to constriction of peripheral arterioles [11]. The contraction of vascular smooth muscle cells (VSMCs) leads to vasoconstriction, with calcium channels expressed on VSMCs playing a crucial role in regulating their contraction [12]. Neurotransmitters or other factors can polarize the cell membrane of VSMCs, resulting in the closure of calcium channels and subsequent reduction in intracellular calcium concentration. This triggers a cascade of biochemical reactions that ultimately lead to vascular dilation [13].

Calcium channels, which are widely distributed in the cell membrane and endoplasmic reticulum, play a crucial role in regulating intracellular calcium concentration and cell membrane potential [14]. Among these channels, L-Type Voltage-gated Calcium Channels (VGCCs) are prevalent in VSMCs and exert significant control over their contraction and relaxation dynamics [13]. Activation of L-Type VGCCs occurs during cellular depolarization, leading to the inflow of extracellular calcium ions and subsequent vasoconstriction mediated by the vascular smooth muscle cells [14, 15]. This regulatory mechanism is essential for maintaining proper vascular function and blood pressure homeostasis.

Inula helenium L., as a species of the Inula genus (Inula spp), is also widely referred to as *Inula racemosa* Hook.f. and *Inula britannica* L. It is included in the Chinese Pharmacopoeia and has various medicinal properties such as expectorant, antitussive, antidiarrheal, antiemetic, and antimicrobial effects, often used in ethnopharmacological research [16]. According to reports, *Inula racemosa* Hook.f. has been found to have beneficial effects on improving atherosclerosis and reducing blood pressure [17, 18]. Alantolactone (ATL), a sesquiterpene lactone compound derived from Inulae Radix, exhibits diverse biological activities including tumor treatment, anti-inflammatory, anti-oxidation, and anti-microbial effects [19]. ATL can ameliorate myocardial ischemia (MI)-induced damage by mitigating oxidative stress, apoptosis, calcium overload, and mitochondrial damage [20]. These findings suggest that ATL holds potential as a protective agent against cardiovascular diseases; however, no studies have reported its efficacy in treating hypertension.

To clarify the therapeutic effect and underlying mechanism of ATL in treating hypertension, we first utilized network pharmacology to predict the associated targets and biological processes involved in ATL's effectiveness against hypertension. Next, we established a mouse model of hypertension by subcutaneously implanting an Ang II sustained release pump to assess the influence of ATL on hypertensive conditions. Lastly, we conducted vascular ring and molecular docking experiments to elucidate the mechanism of action responsible for ATL's antihypertensive effect, which involves inhibiting the activation of L-type VGCCs to suppress intracellular calcium flux.

Materials and methods

Reagents

Alantolactone (Article Number #:B21267, Lot#:Z30S11SS126544, Purity:≥98%) was purchased from Yuanye Biotechnology Co., Ltd (Shanghai, China). Osmotic pumps were purchased from ALZET® (Cupertino, CA, USA). Angiotensin II and phenylephrine were obtained from MedChemExpress (Shanghai, China). Acetylcholine was from Sigma-Aldrich (St. Louis, MO, USA). The primary antibody against α-SMA was purchased from Abcam (Cambridge, MA, USA). CD31(PECAM-1) and pMLC 2 antibodies were obtained from Cell Signaling Technology (Shanghai, China). β-actin antibody, goat anti-mouse IgG and goat anti-rabbit IgG were purchased from Proteintech (Wuhan, China).

Network pharmacology analysis

The co-targets of ATL and Ang II were screened by utilizing the Pharm Mapper database (http://www.lilab-ecust.cn/pharmmapper/) and the Swiss Target

Prediction database (http://swisstargetprediction.ch). The keywords "Alantolactone" and "Angiotensin II" were used to search for targets. Targets with a "z-score" > 0 and "Probability" > 0 were selected. The common targets between ATL and Ang II were then summarized and sorted. The jvenn tool was used to map these common targets, as well as the intersection with hypertension-related targets, to identify potential targets of ATL for the treatment of Ang II-induced hypertension. The protein–protein interaction (PPI) networks of the intersecting targets were constructed using the STRING database (https://string-db.org/) with a medium confidence level (interaction score > 0.40) and visualized using Cytoscape software. The enrichment analyses of the intersecting targets for GO and KEGG pathways were conducted using the DAVID database (https: //david.ncifcrf.gov/) [21]. Enrichment bubble chart and chord plot were performed using the OmicStudio tools at https://www.omicstudio.cn/tool.

Animals

Experimental animals

The animals utilized in this study were C57BL/6 mice aged 8–10 weeks and SD rats weighing 200–300 g. They were housed in a controlled specific pathogen-free (SPF) environment, with an ambient temperature set at 25℃ and a 12-h light/dark cycle. Both the bedding material and feed given to the animals underwent sterilization via Co60 irradiation to guarantee their quality met the SPF standards. All procedures were performed following the ethical guidelines outlined in the Guide for the Care and Use of Laboratory Animals by the National Institutes of Health.

Measurement of internal carotid blood pressure

The mice were anesthetized with tribromoethanol and placed in a supine position on a temperature-controlled pad. Next, the right carotid artery was exposed and the distal segment was ligated using surgical thread, while the proximal segment was tightened with hemostatic forceps. To confirm successful cannulation, a PE-10 catheter was inserted into the right carotid artery and fluctuating blood pressure was measured using a transducer connected to a blood pressure analyzer (BL-420N, TECHMAN). Subsequently, the left jugular vein was exposed and a PE-10 catheter was inserted for drug administration. Each mouse initially received an injection of normal saline, followed by ATL (5 mg/ml, 30 μl) after approximately 20 min [22].

Ang II-induced hypertensive model and administration of ATL

Male C57BL/6 mice were meticulously selected for the study. The experiments were divided into three groups: the Control group, Ang II group, and Ang II + ATL group. Mice in the Ang II and Ang II + ATL groups were anesthetized with isoflurane and positioned in a prone position. The hair in neck and back were shaved and disinfected with iodine. Following this, a 1.5 cm incision was made and a slow-release pump containing Ang II (release rate: 1000 ng/kg/min) was implanted before suturing. In the Control group, a sustained-release pump containing normal saline (release rate: 1000 ng/kg/min) was subcutaneously implanted. The experiment was conducted for a duration of 28 days, during which blood pressure in mice was measured using the tail-cuff method on a weekly basis [23].

Vascular reactivity of the mesenteric arteries

C57BL/6 mice or SD rats were humanely euthanized using CO_2 inhalation. The mesenteric arterial vessels were then extracted and placed in a dish filled with Krebs solution. Under a stereomicroscope, the vessels were promptly cut into 2 mm rings in the Krebs solution. A tungsten wire, approximately 4 cm long, was used to secure the vascular ring to the Multi Myograph System (610 M, Danish Myo Technology A/S, Aarhus N, Denmark), and an initial tension of 3mN was applied and allowed to stabilize for 1 h. Vasoconstriction was induced by adding phenylephrine (Phe) at a concentration of 10 μM. After about 20 min, vasodilation was initiated by introducing acetylcholine (Ach) at a concentration of 10 μM. The effect of ATL on vasodilation in isolated mesenteric artery rings was investigated. Careful selection was made to ensure the use of highly reactive and functional vascular rings. A stimulus of 10^{-5} M Phe was added for stabilization, followed by sequential administration of ATL at concentrations of 10^{-9} M, 10^{-8} M, 10^{-7} M, 10^{-6} M, and 10^{-5} M with a 2-min interval between each concentration. Additionally, ATL at concentrations of 1 μM and 10 μM was added to well-reactive and functional vascular rings for a duration of 30 min. Subsequently, Ang II or Phe at concentrations of 10^{-9} M, 10^{-8} M, 10^{-7} M, 10^{-6} M, and 10^{-5} M were introduced sequentially into each channel with a 2-min interval. In order to assess the impact of ATL on Ca^{2+}-induced constriction in mesenteric artery rings, the rings were incubated with ATL at concentrations of 1 μM and 10 μM for a period of 30 min. Following the incubation, $CaCl_2$ at concentrations of 0.1 mM, 0.25 mM, 0.5 mM, 0.75 mM, 1 mM, 2 mM, and 5 mM, or BAY K 8644 at concentrations of 10^{-10} M, 10^{-9} M, 10^{-8} M, 10^{-7} M, and 10^{-6} M, was added to the rings with a 2-min interval between each concentration. Changes in vascular tension were recorded [22].

Cell culture

Cell culture and treatment

The Rat Aortic Smooth Muscle Cells (RASMCs) were extracted and isolated using aseptic techniques based on established protocols described in the literature [24]. Subsequently, the isolated RASMCs were seeded onto culture dishes and incubated until they reached full confluence. Afterwards, the cells were washed twice with sterile PBS, subjected to trypsin–EDTA digestion when they became rounded, and then terminated by adding complete medium. The digested cells were gently resuspended in complete medium after centrifugation at 800 rpm/min for 3 min and the supernatant was discarded. Finally, subculturing was performed by evenly distributing cells from the P2-P4 generations into three equally sized dishes.

The experiments comprised four groups, namely the control group, ATL group, Ang II group, and Ang II + ATL group, with three wells in each group. The RASMCs that had been digested were then seeded into 6-well plates at a density of approximately 65 to 75%. After a 12-h period of adherence, the medium was replaced with serum-free medium for a 12-h starvation period. The ATL group and Ang II + ATL group underwent pre-treatment with 1 μM ATL for six hours. Subsequently, the Ang II group and Ang II + ATL group were exposed to an additional concentration of 1 μM Ang II for an additional 24 h.

The impact of ATL on calcium influx

The experiments were divided into three groups: Ang II group, Ang II + 1 μM ATL group, and Ang II + 10 μM ATL group, each consisting of three wells. RASMCs were digested and seeded onto Confocal dishes at a density of approximately 65 to 75%. After 12 h of adherence, the medium was replaced with 0.5μL Fluo-4 AM solution to achieve a final concentration of 1 μM. The cells were then incubated at 37°C for one hour. Following this incubation period, the Ang II + 1 μM ATL group and Ang II + 10 μM ATL group were respectively pre-treated with 1 μM ATL and 10 μM ATL for thirty minutes. Confocal microscope settings were adjusted accordingly to capture continuous images while 1 μM Ang II was added to stimulate calcium influx. The resulting green fluorescence generated by Ca^{2+} influx was recorded and preserved [22].

Western blotting

Western blot analysis was performed according to standard protocols [25]. Briefly, cells were washed twice with PBS before adding protein lysate and lysing for 30 min. The lysates were then centrifuged to remove the supernatant, and the protein concentration was determined using the BCA kit. Next, 20 μg of proteins per group were subjected to polyacrylamide gel electrophoresis. The separated proteins were transferred onto nitrocellulose filters and blocked with 10% skim milk powder at room temperature for 1 h. Subsequently, primary antibodies were incubated overnight at 4°C, followed by incubation with secondary antibodies at room temperature for 1 h. Membranes containing protein bands were visualized using an enhanced chemiluminescence (ECL) system (Tanon 5200, China). The band intensities were quantified using Image J software (NIH). The original gel images have been provided in supplementary file (Fig.S2).

H&E staining and immunofluorescence staining

The thoracic aorta, measuring 1–2 cm in length, was excised and fixed in 4% paraformaldehyde for 24 h. Subsequently, the tissue was dehydrated in 20% sucrose for over 48 h. Afterwards, the tissue was embedded with OCT compound and sectioned into 5 μm thick slices using a freezing microtome. These sections were then mounted onto slides and stored at −20℃ until further analysis. H&E staining and immunofluorescence techniques were performed following standard procedures. DAPI was used as a nuclear counterstain [25].

Molecular docking

The PDB database (https://www.rcsb.org) was accessed to retrieve the structure of the voltage-gated calcium channel. To focus on the protein, water molecules, ligands, and other extraneous components were removed. The ATL structure in mol2 file format was obtained. Molecular docking analysis was carried out using the Auto Dock Tools software, and the docking results were visualized using PyMOL software [22].

Statistical analysis

The data from the experiment were analyzed using GraphPad Prism 10.0 software. The results were expressed as the mean ± standard error. Student's t-test was used to compare differences between two groups of data, and One-way ANOVA was used to analyze differences among multiple groups of data. A significance level of $P < 0.05$ was considered statistically significant.

Graphical abstract drawing

The graphical abstract was created with MedPeer (medpeer.cn).

Results

Network pharmacology predicts mechanisms for ATL improves hypertension

Using the Pharm Mapper and Swiss Target Prediction databases, we identified 120 target genes for ATL and 323 target genes for Ang II. The intersection of these

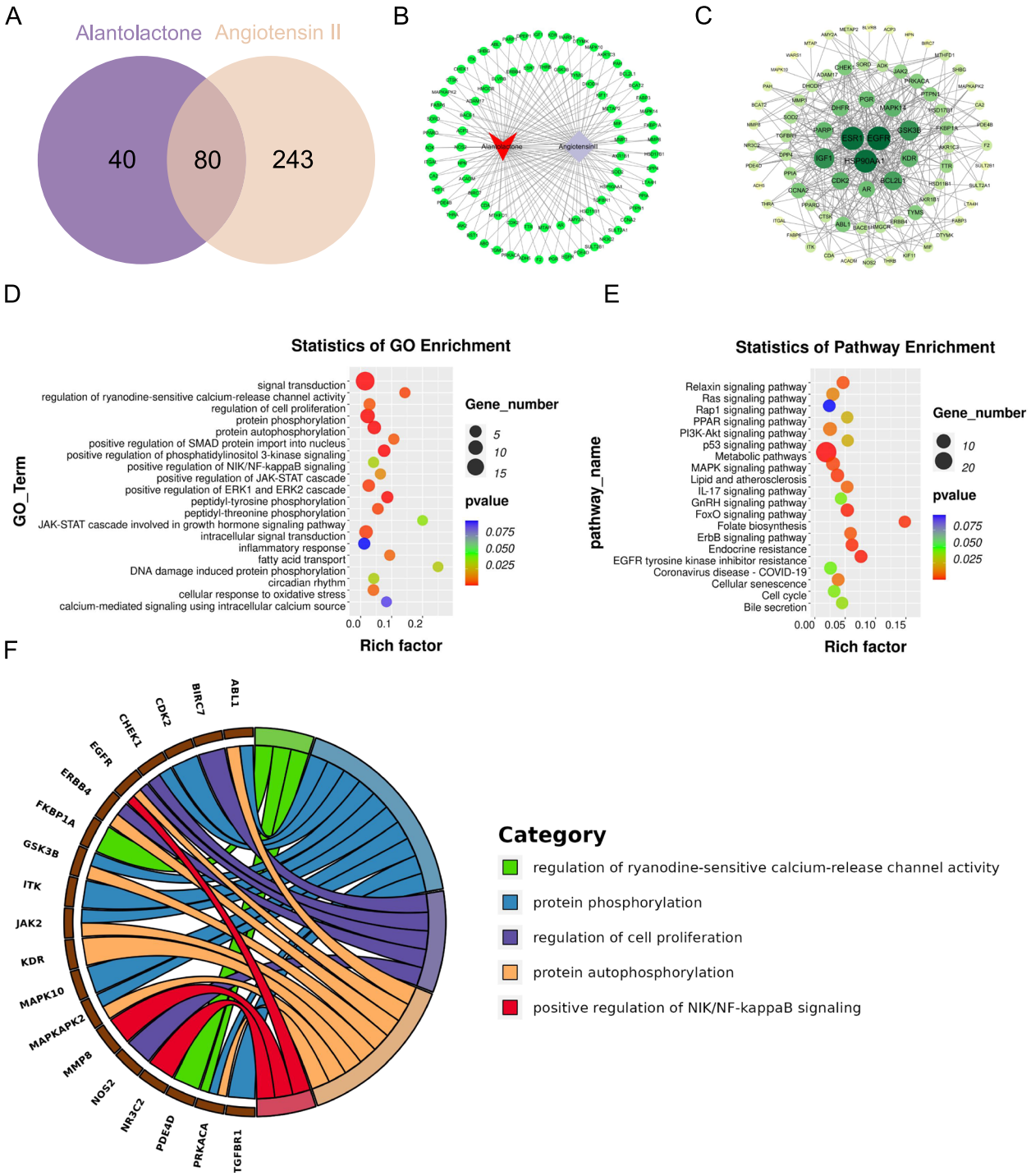

Fig. 1 Predicting the mechanism of ATL in hypertension treatment through network pharmacology. **A** Intersection between ATL targets and Ang II targets. **B** Network of "ATL-target gene-Ang II", red V-shaped represents ATL, gray diamond represents Ang II, and green circles represent common target genes. **C** Network of ATL and Ang II core targets, color shades and circular size represents the degree of node value, the greater the degree value, the deeper the color, the bigger the circle. **D** GO function analysis of biological process (BP) results. **E** Results of KEGG analysis. **F** Chord plot of key pathway-gene enrichment

two sets yielded 80 common target genes shared by both ATL and Ang II (Fig. 1A). To visualize the interaction network of ATL, Ang II, and the common target genes, we utilized Cytoscape v3.10.1 software. In the network, ATL was represented by red V-shapes, Ang II by gray diamonds, and the common target genes by green circles (Fig. 1B). The protein interaction analysis was performed using the String database, resulting in a network graph with 80 nodes and 347 edges. Cytoscape v3.10.1 software was employed to visualize this graph, with larger circles indicating closer arrangement to the center, signifying stronger interactions (Fig. 1C). We conducted GO and KEGG pathway enrichment analysis of the 80 common targets using the DAVID database. The results indicated that ATL and Ang II gene targets were enriched in pathways associated with crucial biological processes, including protein phosphorylation, cell proliferation, inflammatory response, and calcium channels (Fig. 1D). Moreover, signaling pathways such as FoxO, MAPK, Relaxin, ErbB, PI3K-Akt, and IL-17 were identified (Fig. 1E). A closer examination of key biological processes involving calcium channel regulation and protein phosphorylation was pursued (Fig. 1F). In summary, the network pharmacology analysis demonstrated that ATL exerts therapeutic effects on Ang II-induced hypertension.

ATL reduced blood pressure in both normal and hypertensive mice

To validate the hypotensive effects of ATL, we measured the mean arterial pressure in anesthetized mice following intravenous injection of ATL at a concentration of 5 mg/ml, using a volume of 30 µl. The results indicated a rapid but short-term decrease in mouse blood pressure after administration, followed by a quick return to baseline (Fig. 2A-C). These findings suggest that ATL

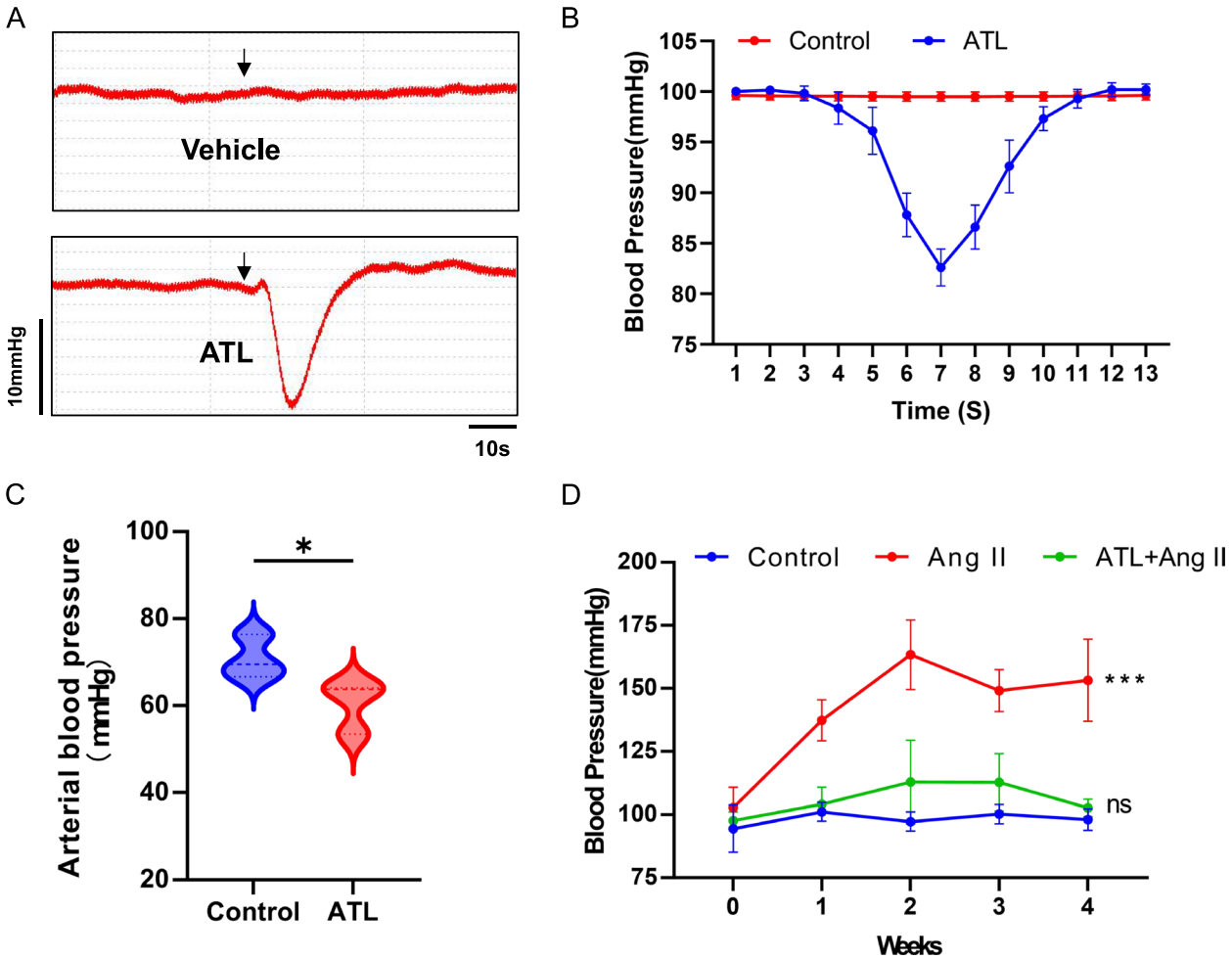

Fig. 2 ATL significantly reduced basal blood pressure and Ang II-induced hypertension in mice. **A**, **B** Carotid artery blood pressure monitoring results. **C** Statistical analysis of the lowest arterial blood pressure values in mice after intravenous treatment. *$P < 0.05$, $n = 4$. **D** ATL improved hypertension induced by Ang II. The experiment begins at week 0, and blood pressure is measured every 7 days for weeks 1–4. ***$P < 0.001$, $n = 5–7$

can indeed affect mouse blood pressure. To further investigate the hypotensive effect of ATL, we implanted sustained release pumps subcutaneously in mice. The treatment group received daily oral administration of ATL, and we assessed the blood pressure of the mice on a weekly basis. The results showed that, compared to the control groups, the blood pressures of the Ang II group started to rise from week one, peaked during week two, and then slightly decreased but remained significantly different from the controls. However, mice treated with ATL exhibited a significant reduction in blood pressure compared to the model group (Fig. 2D). This suggests that ATL has the potential to be an effective therapy for ameliorating Ang II-induced hypertension.

ATL inhibited vasoconstriction

To further clarify the hypotensive effect of ATL, a vascular ring assay was performed to assess its effect on vasoconstriction and vasodilation. Experimental results showed that different concentrations of ATL did not produce relaxation in phenylephrine-induced vasoconstriction in comparison to the control group (Fig. 3A, B). This suggested that ATL did not have a significant vasorelaxant effect. To investigate whether ATL can inhibit vasoconstriction induced by Ang II, the vessels were pretreated with ATL (1 μM or 10 μM) for 30 min before the stimulation with various concentrations of Ang II. The results demonstrated that ATL significantly inhibited Ang II-induced vasoconstriction (Fig. 3C, D). Furthermore, the effect of ATL on vasoconstriction induced by Phe was examined. The results showed that pretreatment with 1 μM and 10 μM ATL for 30 min significantly attenuated the increase in vascular tone induced by Phe (Fig. 3E, F). Calcium ion plays a crucial role in vasoconstriction. To elucidate the regulatory effect of ATL on Ca^{2+} influx, the vessels were preincubated with 1 μM and 10 μM ATL for 30 min and then stimulated with various concentrations of Ca^{2+} to induce vasoconstriction. The experimental results demonstrated that after pretreatment with ATL, blood vessels could still contract upon the addition of Ca^{2+}, but the magnitude of contraction was significantly lower than that of the control group (Fig. 3G, H). We conducted the same experiment using rat mesenteric arteries and obtained consistent results (Fig. S1). These findings indicate that ATL effectively inhibits vasoconstriction induced by Ang II, Phe, and Ca^{2+}. Importantly, no impact on vasodilation was observed.

ATL inhibited Ang II-induced calcium influx

The RASMCs were pretreated with 1 μM and 10 μM ATL for 30 min. After that, Ang II was added in the presence of Ca^{2+} probes to monitor intracellular Ca^{2+} dynamics. It was observed that in the control group, there was a rapid increase in intracellular calcium concentration upon Ang II administration. This increase was indicated by a sharp rise in green fluorescence intensity, which subsequently declined after reaching a critical point. However, treatment with both 1 μM and 10 μM ATL significantly attenuated the Ang II-induced calcium influx in RASMCs, resulting in reduced fluorescence intensity (Fig. 4A-C). These results demonstrate that ATL is able to inhibit Ang II-induced calcium influx in RASMCs. The increase in calcium influx in vascular smooth muscle cells leads to an increase in MLC2 phosphorylation, which in turn induces smooth muscle contraction. To confirm the effect of ATL on MLC2 phosphorylation, Western Blotting was utilized. Experimental findings showed that, compared to the control group, Ang II significantly upregulated MLC2 phosphorylation in RASMCs after 24 h of treatment. However, ATL did not have a significant impact on MLC2 phosphorylation in RASMCs. Nevertheless, pretreatment with ATL effectively inhibited Ang II-induced increases in MLC2 phosphorylation in RASMCs (Fig. 4D, E).

ATL inhibited calcium influx by inhibiting L-type calcium channel activation

To investigate the inhibition of calcium ion influx by ATL through its interaction with calcium ion channels, we performed docking experiments using ATL as a ligand against voltage-gated calcium channels (VGCCs) proteins. Subsequently, we analyzed the resulting molecular docking affinity values. The molecular docking results revealed that L-type VGCCs exhibited ATL affinity values below −5 kcal/mol, indicating a strong binding activity between ATL and these proteins (Fig. 5A). To evaluate the inhibitory effect of ATL on L-type VGCCs, mesenteric arteries were exposed to varying concentrations of ATL for 30 min, followed by the induction of contraction using the L-type VGCCs activator BAY K 8644. The results demonstrated a concentration-dependent reduction in BAY K 8644-induced vasoconstriction upon treatment with ATL (Fig. 5B, C). These findings suggest that ATL exerts its inhibitory action on calcium influx through modulation of L-type VGCCs.

ATL improved Ang II-induced vascular hypertrophy

H&E staining revealed that the Ang II group exhibited a thickened vascular wall with a significant increase in proliferative cells between elastic fibers, compared to the control group. However, treatment with ATL significantly improved the Ang II-induced vascular wall thickening (Fig. 6A, B). Immunofluorescence staining showed that Ang II induced extensive proliferation of vascular smooth

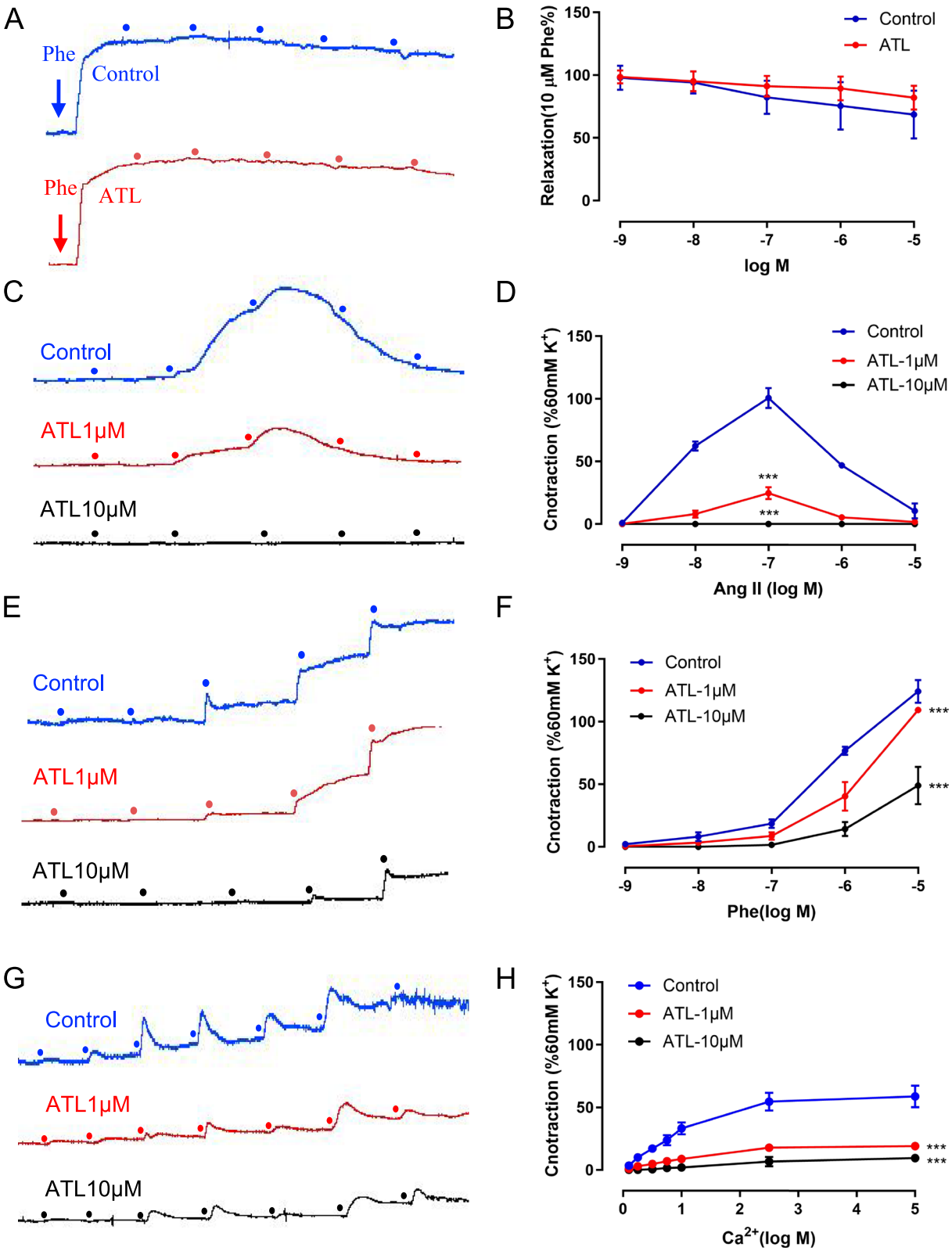

Fig. 3 Effects of ATL on vasodilation and contraction. **A**, **B** ATL does not impact the diastolic function of the mesenteric artery. **C**, **D** ATL inhibits Ang II-induced vasoconstriction. **E**, **F** ATL inhibits Phe-induced vasoconstriction. **G**, **H** ATL inhibits Ca^{2+}-induced vasoconstriction. ***$P < 0.001$, $n = 4$

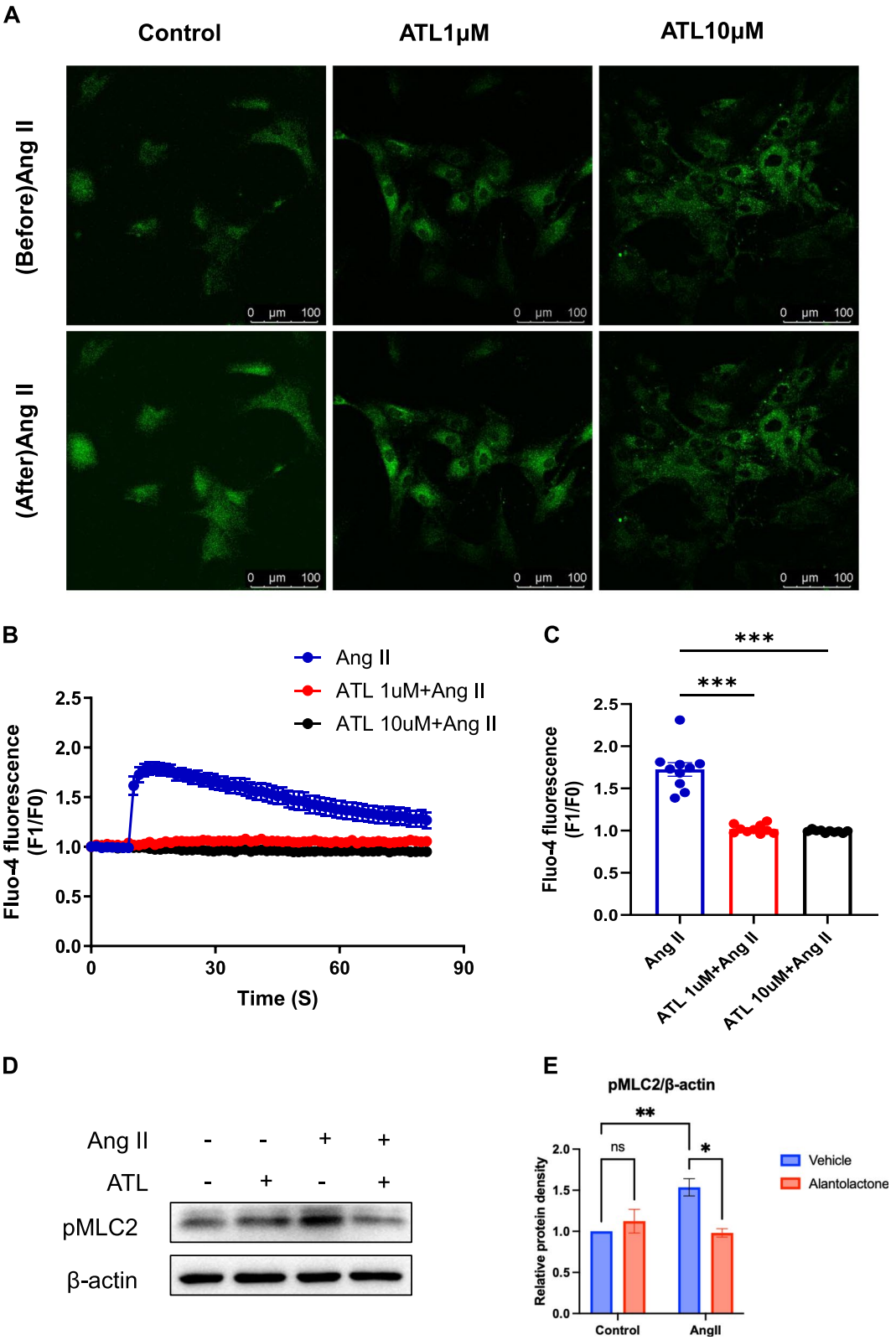

Fig. 4 ATL inhibited Ang II-induced calcium influx and the upregulation of pMLC2 in RASMCs. **A** Fluorescence intensity of calcium probe before and after administration of Ang II in different treatment groups. **B** Statistical plot of fluorescence intensity changes over time in different groups. **C** Statistical plot of the strongest values of fluorescence after the addition of Ang II. ***$P < 0.001$, $n = 10$. **D** Western Blotting representative plots of pMLC2 of cells in different treatment groups. **E** Statistical analysis of the results shown in (**D**). *$P < 0.05$, $n = 3$

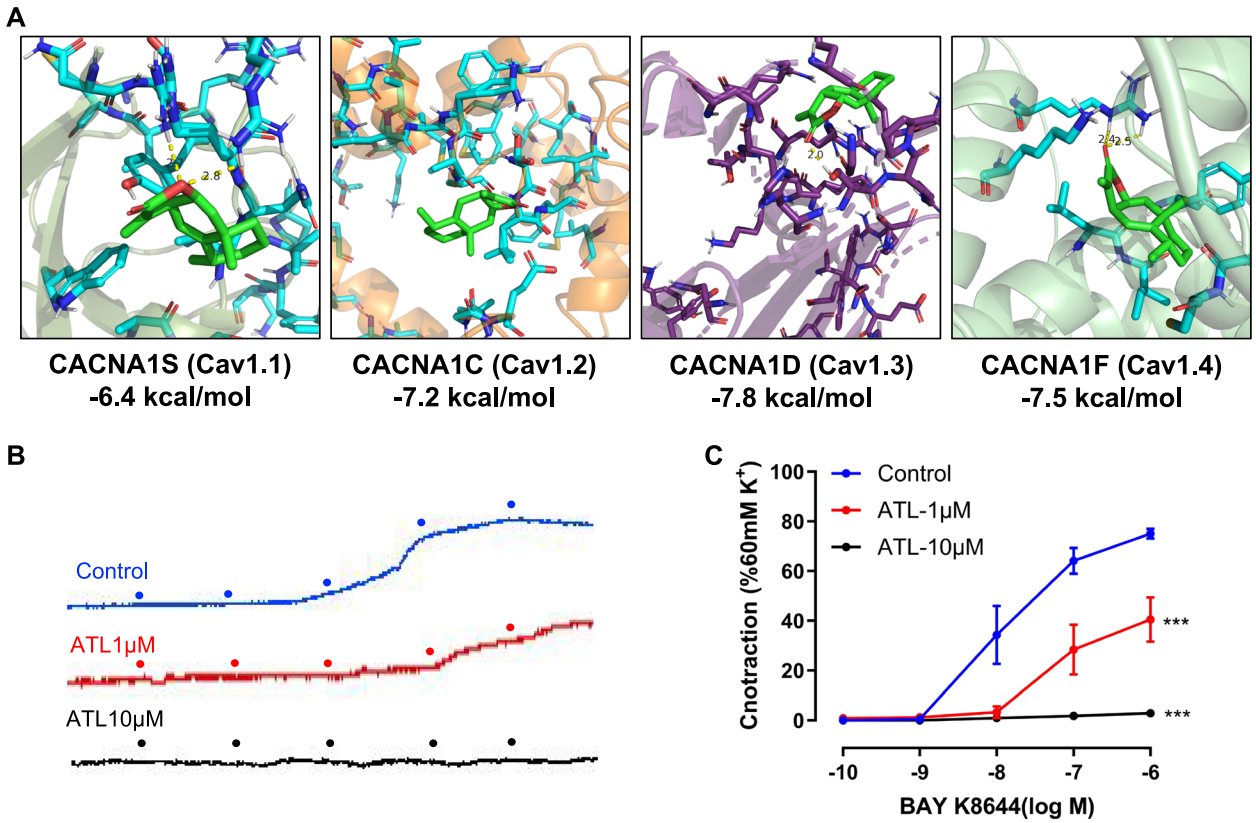

Fig. 5 ATL inhibition of L-type VGCCs. **A** Results of docking between ATL and L-type VGCCs. **B** ATL inhibits BAY K 8644-induced vasoconstriction. ***$P < 0.001$, $n = 4$

muscle cells. In contrast, ATL treatment effectively inhibited this process (Fig. 6C).

Discussion

ATL is a sesquiterpene lactonide compound that can be found in various plants, particularly in Inula helenium. Previous studies have investigated the pharmacological activities of ATL, including its anti-tumor, anti-inflammatory, and antibacterial properties, as well as its potential for treating skin diseases [26, 27]. However, there is currently no research on its efficacy in the treatment of hypertension. The etiology of hypertension is complex, and Ang II is a key factor in the elevation of blood pressure [10]. Therefore, we considered the target of Ang II as the main target for drug treatment of hypertension, and Ang II was used to induce hypertension in both cell and animal experiments. Through network pharmacology analysis, we discovered multiple common target proteins shared by ATL and Ang II. Notably, the key targets of ATL include EGFR, GSK3B, ERBB4, and PRKACA, which are involved in various biological processes such as cell proliferation, regulation of inflammation, and calcium channel activity.

VSMCs are highly specialized cells responsible for regulating blood flow and blood pressure through contraction [28]. In response to various stimuli VSMCs undergo a phenotypic switch from differentiation to dedifferentiation, which plays a crucial role in the pathophysiology of vascular remodeling associated with hypertension [29]. Ang II induces contraction, proliferation, and hypertrophy of vascular smooth muscle cells within the vascular wall, thereby contributing to the development of hypertension [30, 31]. Consistent with previous literature, our study demonstrated that Ang II promoted extensive proliferation of VSMCs and triggered vascular remodeling. Notably, this effect was reversed by ATL treatment. These findings suggest that ATL has potential therapeutic benefits for hypertension by suppressing excessive proliferation of VSMCs.

Calcium ions play a critical role in the normal physiological function of cells. In various disease signaling pathways, Ca^{2+} is commonly used as a mediator or regulatory target to modulate cellular functions [32]. The increase in calcium ion concentration in VSMCs acts as the primary inducer of vasoconstriction and also stimulates smooth muscle cell proliferation and

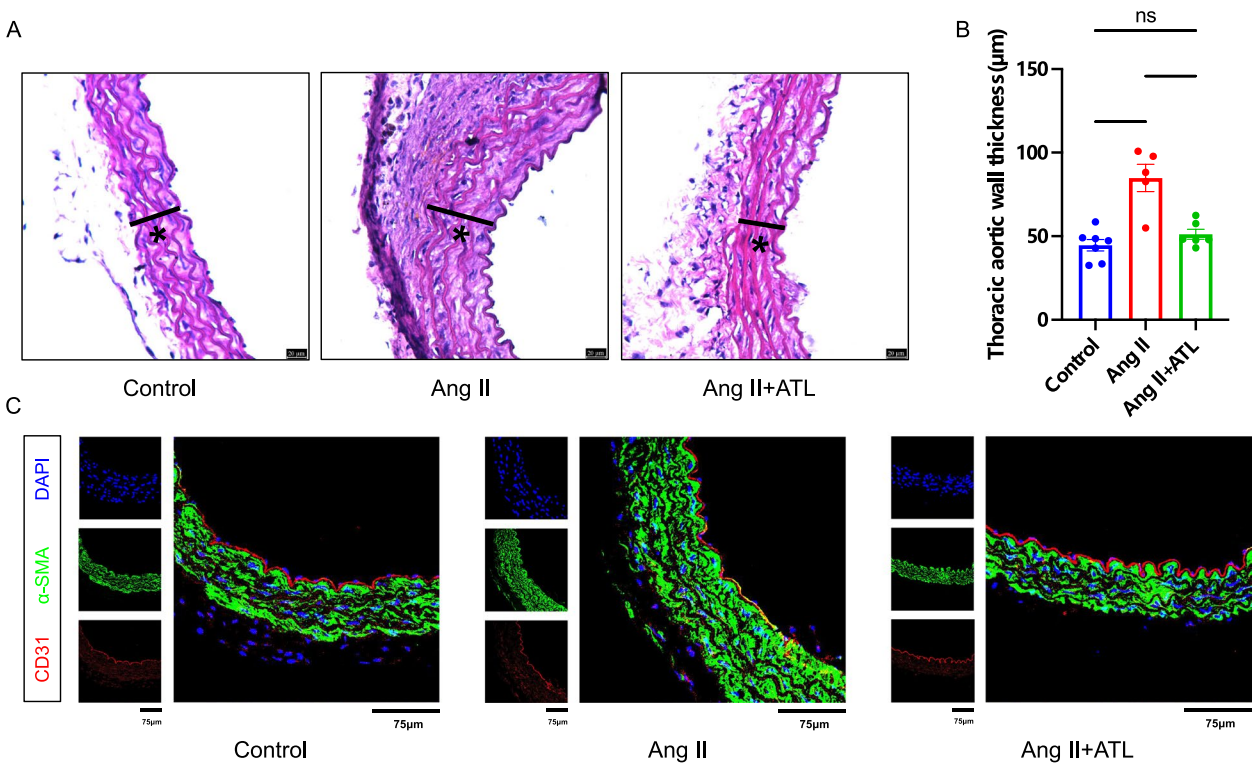

Fig. 6 Results of H&E and immunofluorescence staining of the mouse thoracic aorta. **A** Results of H&E staining of mouse thoracic aorta, cytoplasmic and extracellular matrix-stained components are shown in red, nuclei in blue, * represents vessel wall thickness, and ruler length is 20 μm. **B** Statistical analysis of H&E staining. **C** immunofluorescence staining of the mouse thoracic aorta. Endothelial cell marker CD31 in red, vascular smooth muscle cell marker α-SMA in green, and nucleus in blue. The ruler length is 75 μm

migration [33]. The elevation of intracellular calcium primarily occurs through the release of calcium stores, such as the sarcoplasmic reticulum (SR) and endoplasmic reticulum (ER), along with extracellular influx through ion channels [34]. L-type VGCCs are widely distributed in vascular smooth muscles and significantly influence their contraction-relaxation dynamics [14]. These VGCCs consist of four main subunits: the α1 subunit and auxiliary subunits β, α2δ, and γ [35]. L-type VGCCs open during cell depolarization, leading to the influx of extracellular calcium ions and subsequent vasoconstriction mediated by VSMCs [36]. In this study, we discovered that ATL inhibited Ang II, Phe, and Ca^{2+}-induced constriction of vascular rings. Cell experiments demonstrated that Ang II promoted Ca^{2+} influx and increased the protein level of p-MLC2 in RASMCs, while ATL inhibited Ca^{2+} influx and p-MLC2 protein level. Furthermore, ATL exhibited strong binding affinity with L-type VGCCs proteins including Cav1.1, Cav1.2, Cav1.3, and Cav1.4. Subsequently, we added the L-type VGCCs activator BAY K 8644 to the vascular ring experiment, and the results showed that ATL could indeed inhibit vascular constriction caused by BAY K 8644. These findings suggest that ATL can suppress Ang II-induced calcium influx and MLC phosphorylation in VSMCs by targeting cellular L-type VGCCs.

Long-term stimulation of Ang II can cause vascular smooth muscle proliferation, resulting in thickening and remodeling of the vascular wall [37, 38]. Therefore, we examined the vessel morphology during the experiment. The results from H&E and immunofluorescence staining demonstrated that ATL effectively protected the vessels and inhibited Ang II-induced vascular remodeling.

Conclusion

In conclusion, ATL could effectively reduce the elevation of blood pressure caused by Ang II. ATL inhibited calcium influx and the phosphorylation of MLC2 by binding to L-type VGCCs, thereby suppressing the vascular contraction induced by Ang II. Our research had not only identified the antihypertensive effect of alantolactone but also elucidated its mechanism of action. Meanwhile, our study had provided a basis for the development of new drugs for the treatment of hypertension.

Abbreviations

Ang II	Angiotensin II
CO	Cardiac Output

TPR	Total Peripheral Resistance
RAAS	Renin Angiotensin-Aldosterone System
VSMCs	Vascular Smooth Muscle Cells
VGCCs	Voltage-gated Calcium Channels
ATL	Alantolactone
MI	Myocardial ischemia
TC	Total cholesterol
TG	Triglyceride
PPI	Protein-protein interaction
SPF	Specific pathogen-free
Phe	Phenylephrine
Ach	Acetylcholine
RASMCs	Rat Aortic Smooth Muscle Cells
ECL	Enhanced chemiluminescence
H&E staining	Hematoxylin-Eosin Staining
SD rat	Sprague-Dawley rat
ER	Endoplasmic reticulum

Supplementary Information

The online version contains supplementary material available at https://doi.org/10.1186/s12872-024-04461-2.

Supplementary Material 1.

Supplementary Material 2.

Acknowledgements
Not applicable.

Authors' contributions
Ruqiang Yuan, Mingjing Gao and Hu Xu: Conceived and designed the experiments. Ruqiang Yuan, Houli Zhang and Qing Liang: performed the biological experiments and phytochemical analysis. Erjiao Qiang, Lei Qian and Yali Wang: calculated and supervised the study. Hu Xu and Weijing Yun: drafted the manuscript. All authors read and approved the final manuscript.

Funding
This work was supported by the Scientific Research Fund Project of Liaoning Provincial Department of Education (LJ212410161002, LJKMZ20221267).

Data availability
No datasets were generated or analysed during the current study.

Declarations

Ethics approval and consent to participate
The animal study was reviewed and approved by Ethics Committee of Dalian Medical University.

Competing interests
The authors declare no competing interests.

Author details
[1]Advanced Institute for Medical Sciences, Dalian Medical University, Dalian 116044, China. [2]Department of Pharmacy, Dalian Port Hospital, Dalian 116001, China. [3]College of Pharmacy, Dalian Medical University, Dalian 116044, China. [4]Wuhu Hospital and Health Science Center, East China Normal University, Shanghai 200241, China. [5]Department of Pathology, Shanghai General Hospital, Shanghai Jiaotong University School of Medicine, Shanghai 200080, China.

Received: 7 November 2024 Accepted: 30 December 2024
Published online: 06 January 2025

References

1. Carretero OA, Oparil S. Essential hypertension. Part I: definition and etiology Circulation. 2000;101(3):329–35.
2. Manosroi W, Williams GH. Genetics of human primary hypertension: focus on hormonal mechanisms. Endocr Rev. 2019;40(3):825–56.
3. Boulestreau R, van den Born BH, Lip GYH, Gupta A. Malignant hypertension: current perspectives and challenges. J Am Heart Assoc. 2022;11(7):e023397.
4. Elliott WJ. Systemic hypertension. Curr Probl Cardiol. 2007;32(4):201–59.
5. Pierdomenico SD, Di Nicola M, Esposito AL, Di Mascio R, Ballone E, Lapenna D, Cuccurullo F. Prognostic value of different indices of blood pressure variability in hypertensive patients. Am J Hypertens. 2009;22(8):842–7.
6. Li X, Bijlsma MJ, Bos JHJ, Schuiling-Veninga CCM, Hak E. Long-term comparative effectiveness of antihypertensive monotherapies in primary prevention of cardiovascular events: a population-based retrospective inception cohort study in the Netherlands. BMJ Open. 2023;13(8):e068721.
7. Shin J, Chia YC, Heo R, Kario K, Turana Y, Chen CH, Hoshide S, Fujiwara T, Nagai M, Siddique S, et al. Current status of adherence interventions in hypertension management in Asian countries: A report from the HOPE Asia Network. J Clin Hypertens (Greenwich). 2020;23(3):584–94.
8. Messerli FH, Bangalore S, Bavishi C, Rimoldi SF. Angiotensin-converting enzyme inhibitors in hypertension: to use or not to use? J Am Coll Cardiol. 2018;71(13):1474–82.
9. Magder S. The meaning of blood pressure. Critical care (London, England). 2018;22(1):257.
10. Patel S, Rauf A, Khan H, Abu-Izneid T. Renin-angiotensin-aldosterone (RAAS): The ubiquitous system for homeostasis and pathologies. Biomed Pharmacother. 2017;94:317–25.
11. Falkner B. Cardiac output versus total peripheral resistance. Hypertension. 2018;72(5):1093–4.
12. Lorigo M, Oliveira N, Cairrao E. Clinical importance of the human umbilical artery potassium channels. Cells. 2020;9(9):1956.
13. Zamponi GW, Striessnig J, Koschak A, Dolphin AC. The physiology, pathology, and pharmacology of voltage-gated calcium channels and their future therapeutic potential. Pharmacol Rev. 2015;67(4):821–70.
14. Catterall WA. Voltage-gated calcium channels. Cold Spring Harb Perspect Biol. 2011;3(8):a003947.
15. Morad M, Soldatov N. Calcium channel inactivation: possible role in signal transduction and Ca2+ signaling. Cell Calcium. 2005;38(3–4):223–31.
16. Seca AM, Grigore A, Pinto DC, Silva AM. The genus Inula and their metabolites: from ethnopharmacological to medicinal uses. J Ethnopharmacol. 2014;154(2):286–310.
17. Mangathayaru K, Kuruvilla S, Balakrishna K, Venkhatesh J. Modulatory effect of Inula racemosa Hook. f. (Asteraceae) on experimental atherosclerosis in guinea-pigs. J Pharm Pharmacol. 2009;61(8):1111–8.
18. Rathore S, Raj Y, Debnath P, Kumar M, Kumar R. Ethnopharmacology, phytochemistry, agrotechnology, and conservation of Inula racemosa Hook f. - A critically endangered medicinal plant of the western Himalaya. J Ethnopharmacol. 2022;283:114613.
19. Liu X, Bian L, Duan X, Zhuang X, Sui Y, Yang L. Alantolactone: A sesquiterpene lactone with diverse pharmacological effects. Chem Biol Drug Des. 2021;98(6):1131–45.
20. Liu M, Liu P, Zheng B, Liu Y, Li L, Han X, Liu Y, Chu L. Cardioprotective effects of alantolactone on isoproterenol-induced cardiac injury and cobalt chloride-induced cardiomyocyte injury. Int J Immunopathol Pharmacol. 2022;36:20587384211051990.
21. Zhou W, Zhang H, Wang X, Kang J, Guo W, Zhou L, Liu H, Wang M, Jia R, Du X, et al. Network pharmacology to unveil the mechanism of Moluodan in the treatment of chronic atrophic gastritis. Phytomedicine. 2022;95: 153837.
22. Yun WJ, Zhang XY, Liu TT, Liang JH, Sun CP, Yan JK, Huo XK, Tian XG, Zhang BJ, Huang HL, et al. The inhibition effect of uncarialin A on voltage-dependent L-type calcium channel subunit alpha-1C: Inhibition potential and molecular stimulation. Int J Biol Macromol. 2020;159:1022–30.
23. Yuan RQ, Qian L, Yun WJ, Cui XH, Lv GX, Tang WQ, Cao RC, Xu H. Cucurbitacins extracted from Cucumis melo L. (CuEC) exert a hypotensive effect via regulating vascular tone. Hypertens Res. 2019;42(8):1152–61.
24. Trufanov SK, Rybakova EY, Avdonin PP, Tsitrina AA, Zharkikh IL, Goncharov NV, Jenkins RO, Avdonin PV. The role of two-pore channels in

norepinephrine-induced [Ca(2+)](i) rise in rat aortic smooth muscle cells and aorta contraction. Cells. 2019;8(10):1144.
25. Xu H, Du S, Fang B, Li C, Jia X, Zheng S, Wang S, Li Q, Su W, Wang N, et al. VSMC-specific EP4 deletion exacerbates angiotensin II-induced aortic dissection by increasing vascular inflammation and blood pressure. Proc Natl Acad Sci USA. 2019;116(17):8457–62.
26. Cai Y, Gao K, Peng B, Xu Z, Peng J, Li J, Chen X, Zeng S, Hu K, Yan Y. Alantolactone: a natural plant extract as a potential therapeutic agent for cancer. Front Pharmacol. 2021;12:781033.
27. Mi XG, Song ZB, Wu P, Zhang YW, Sun LG, Bao YL, Zhang Y, Zheng LH, Sun Y, Yu CL, et al. Alantolactone induces cell apoptosis partially through down-regulation of testes-specific protease 50 expression. Toxicol Lett. 2014;224(3):349–55.
28. Khachigian LM, Black BL, Ferdinandy P, De Caterina R, Madonna R, Geng YJ. Transcriptional regulation of vascular smooth muscle cell proliferation, differentiation and senescence: Novel targets for therapy. Vascul Pharmacol. 2022;146:107091.
29. Frismantiene A, Philippova M, Erne P, Resink TJ. Smooth muscle cell-driven vascular diseases and molecular mechanisms of VSMC plasticity. Cell Signal. 2018;52:48–64.
30. De Mello WC. Intracellular angiotensin II as a regulator of muscle tone in vascular resistance vessels. Pathophysiological implications. Peptides. 2016;78:87–90.
31. Zhang F, Ren X, Zhao M, Zhou B, Han Y. Angiotensin-(1–7) abrogates angiotensin II-induced proliferation, migration and inflammation in VSMCs through inactivation of ROS-mediated PI3K/Akt and MAPK/ERK signaling pathways. Sci Rep. 2016;6:34621.
32. Dolphin AC. Calcium channel diversity: multiple roles of calcium channel subunits. Curr Opin Neurobiol. 2009;19(3):237–44.
33. Chen Z, Zhou Q, Chen J, Yang Y, Chen W, Mao H, Ouyang X, Zhang K, Tang M, Yan J, et al. MCU-dependent mitochondrial calcium uptake-induced mitophagy contributes to apelin-13-stimulated VSMCs proliferation. Vascul Pharmacol. 2022;144:106979.
34. Zhou X, Lin P, Yamazaki D, Park KH, Komazaki S, Chen SR, Takeshima H, Ma J. Trimeric intracellular cation channels and sarcoplasmic/endoplasmic reticulum calcium homeostasis. Circ Res. 2014;114(4):706–16.
35. Xu L, Sun L, Xie L, Mou S, Zhang D, Zhu J, Xu P. Advances in L-type calcium channel structures, functions and molecular modeling. Curr Med Chem. 2021;28(3):514–24.
36. Johnson MT, Gudlur A, Zhang X, Xin P, Emrich SM, Yoast RE, Courjaret R, Nwokonko RM, Li W, Hempel N, et al. L-type Ca(2+) channel blockers promote vascular remodeling through activation of STIM proteins. Proc Natl Acad Sci USA. 2020;117(29):17369–80.
37. Das S, Senapati P, Chen Z, Reddy MA, Ganguly R, Lanting L, Mandi V, Bansal A, Leung A, Zhang S, et al. Regulation of angiotensin II actions by enhancers and super-enhancers in vascular smooth muscle cells. Nat Commun. 2017;8(1):1467.
38. Cau SB, Bruder-Nascimento A, Silva MB, Ramalho FNZ, Mestriner F, Alves-Lopes R, Ferreira N, Tostes RC, Bruder-Nascimento T. Angiotensin-II activates vascular inflammasome and induces vascular damage. Vascul Pharmacol. 2021;139:106881.

Publisher's Note